MULTI-PIXEL PHOTON COUNTER FOR OPERATING A TABLETOP COSMIC RAY DETECTOR UNDER LOOSELY CONTROLLED CONDITIONS

Nguyen Hoang Duy Thanh[a*], Nguyen Vu Chi Lan[a, b], Cao Van Son[a, c], Tran Van Ngoc[a, d], Nguyen Khoa[e], Nguyen Thi Hong Van[f], Phan To Quyen[a, d]

[a]Institute for Interdisciplinary Research in Science and Education (IFIRSE), Binh Dinh, Vietnam
[b]The University of Sheffield, Sheffield, United Kingdom
[c]High Energy Accelerator Research Organization (KEK), Tsukuba, Ibaraki, Japan
[d]Graduate University of Science and Technology, Vietnam Academy of Science and Technology, Hanoi, Vietnam
[e]Albion College, Albion, Michigan, United States
[f]Institute of Physics, Vietnam Academy of Science and Technology, Hanoi, Vietnam
[*]Corresponding author: Email: nhdthanh@ifirse.icise.vn

Article history
Received: December 6th, 2021
Received in revised form: April 19th, 2022 | Accepted: June 30th, 2022
Available online: October 4th, 2022

Abstract

The multi-pixel photon counter (*MPPC*) *has recently emerged as a great type of silicon photomultiplier to replace or compensate for conventional vacuum-based photomultiplier tubes. An MPPC provides many advantageous features, such as high electrical gain, outstanding photon detection efficiency, fast timing response, immunity to magnetic fields, low-voltage operation, compactness, portability, and cost-effectiveness. This article examines the electrical and optical characteristics of an MPPC under loosely controlled environmental conditions. We also report a measurement of the light yield captured by the MPPC when a cosmic ray passes through the plastic scintillator, demonstrating that such a setup is suitable as a simple, cost-effective tabletop cosmic ray detector for educational and research purposes.*

Keywords: Photon detectors for UV, visible, and IR photons (solid-state); Scintillators, scintillation, and light emission processes; Solid state detectors.

DOI: https://doi.org/10.37569/DalatUniversity.13.1.1019(2023)

Article type: (peer-reviewed) Full-length research article

1. INTRODUCTION

In this paper, we investigate the electrical and optical characteristics of an excellent type of single-photon-resolving detector known as a multi-pixel photon counter (MPPC) (Ghassemi et al., 2018). This photodetector has a wide range of both scientific and industrial applications, including, but not limited to, tracking and calorimetry in particle physics, radiation monitoring, medical imaging, light detection and ranging, and quantum computing. In this study, we use this sensor, along with plastic scintillators and wavelength shifting fibers to measure cosmic rays. Notably, we perform these measurements on a laboratory tabletop where the environmental conditions of temperature and humidity are not tightly controlled. This can be problematic because it is well-established that a number of MPPC properties are sensitive to temperature. Therefore, the investigation of the behavior of an MPPC is critical when the operational conditions cannot be well-controlled or when it is difficult to do so.

1.1. Silicon photodiode, avalanche breakdown, and Geiger mode

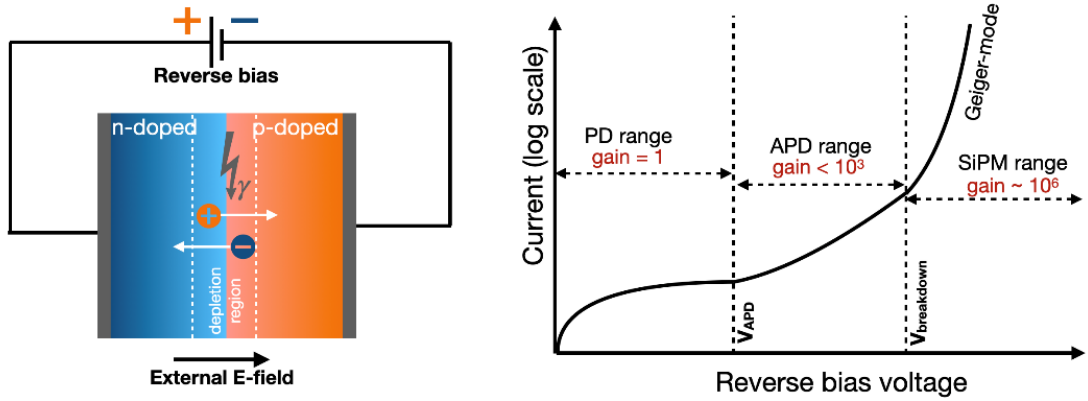

Figure 1. Operational principle of a p-n junction and classification of photodiode (PD), avalanche photodiode (APD), and SiPM operating in the Geiger-mode avalanche

A photodiode, as illustrated on the left in Figure 1, is made from a silicon doped p-n junction that establishes a depletion region of mobile carriers in thermal equilibrium (Neamen, 2011). When a photon is incident on silicon, an electron-hole pair is created via the photoelectric effect in the depletion region. When a reverse-biased voltage is applied to the silicon photodiode, it generates a high electric field across the depletion region. The produced charge carriers experience an increase in kinetic energy and collide with the lattice atoms, eventually losing their energy as thermal phonons. When the applied voltage is high enough, the carriers have sufficient power to ionize the lattice atoms, inducing additional electron-hole pairs and resulting in a chain of ionization called an *avalanche breakdown* or *avalanche multiplication*. Thus, an absorbed photon can trigger a macroscopic electrical current, allowing us to distinctly detect the photon's incidence. A photodiode called an *avalanche photodiode* (APD) is designed to operate in such conditions. The charge collected from the avalanche multiplication is expressed in terms of the electron charge unit and is called the electrical gain. When the operating voltage is lower than the APD breakdown voltage, a turning point is reached where the

silicon suddenly becomes conductive when subjected to an external electric field. The electrical gain has a linear response to the applied voltage and is typically less than one thousand. When the reverse bias voltage exceeds the APD breakdown voltage, the electrical gain increases drastically. The APD becomes a binary response, such that the output charge is independent of the intensity of the incident photons. A silicon photomultiplier (SiPM), the term for the APD operated in the Geiger mode, has an electrical gain of 10^6. The classification of the photodiode, APD, and SiPM based on the amplitude of the reverse bias voltage is illustrated on the right in Figure 1.

1.2. Multi-Pixel Photon Counter

The multi-pixel photon counter developed by Hamamatsu, Japan, (Ghassemi et al., 2018) is one of the most widely used SiPMs. It is fabricated on a monolithic silicon crystal with a composite-metal quenching resistor around each APD, forming a pixel. Multiple pixels are arranged in two dimensions, connected in parallel with a common reverse bias voltage, and read by a united output. An equivalent MPPC circuit and a close-up view of a single MPPC are shown in Figure 2. Since each pixel produces the same electrical current per incident photon, the MPPC signal summing the currents from the fired pixels is equivalent in practice to the number of incident photons, providing the MPPC with an excellent capability to count photons.

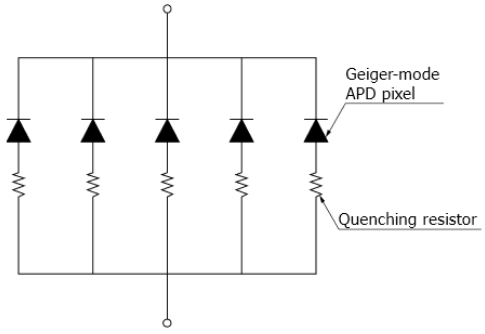

(a)

(b)

Figure 2. (a) An equivalent MPPC circuit with APD pixels connected in parallel; (b) a close-up view of an MPPC with 667 pixels manufactured on a 1.3 x 1.3 mm^2 sensitive area

Sources: (a): Groom et al. (2001); (b): Hamamatsu Photonics (2020).

The first generation of Hamamatsu MPPCs, the S10362 series, was announced in 2007 (Ohashi, 2019). Six years later, the second generation of MPPCs, the S1257x series, was released with lower afterpulse and improved photon detection efficiency (PDE) but still relatively high crosstalk. In 2015, Hamamatsu introduced a new generation of MPPCs, the S13xyz series, with lower crosstalk and afterpulse and higher fill factor. Compared to the S1257x series, this series provides a higher PDE for a broader range of wavelengths from UV to visible light. In 2017, a new lineup of products with excellent coincidence time resolution, the S14160/S14161 series, was released. This series is

dedicated to time-of-flight applications such as positron emission tomography. Recently, two additional product lineups (Yamamoto et al., 2019) have been introduced: (i) the S14520 series designed for Cherenkov telescopes with high PDE in the UV region and (ii) the S14160 series with a pixel size of 10 μm by 15 μm and a new design of the pixel trench, achieving lower noise and crosstalk, higher PDE, wide dynamic range, and lower power consumption.

Figure 3 shows the electrical pulses induced by thermal noise for two generations of MPPCs. The signal was amplified with a NIM amplifier module by a factor of 100 and read out by a Tektronix TBS1104 100 MHz bandwidth digital storage oscilloscope. The electrical pulses with one and two photoelectrons (p.e.) are visually well distinguished for both MPPC generations. The signal rise time is around a few nanoseconds (ns) and the signal decay time is a few tens of nanoseconds.

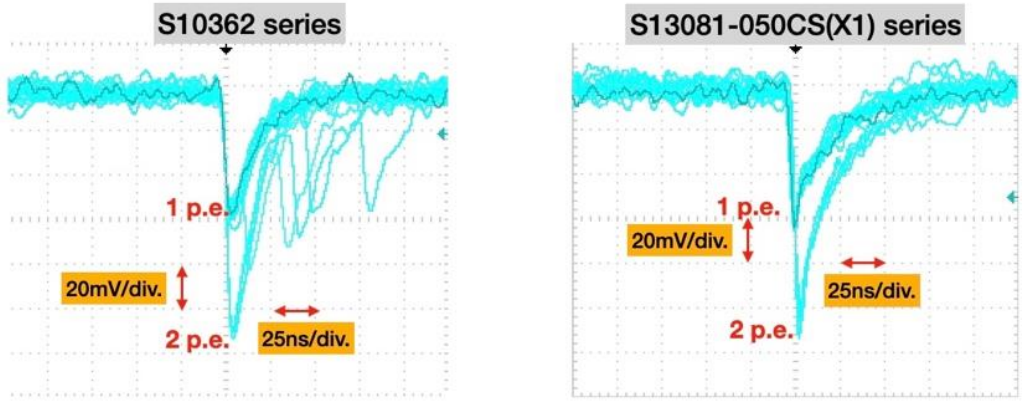

Figure 3. MPPC waveforms for the first (S10362 series) and third (S13081-050CS(X1) series) MPPC generations triggered by thermal noise

Notes: Electrical pulses with one and two photoelectrons (p.e.) are clearly distinct. The third MPPC generation observably suppresses the afterpulse and crosstalk.

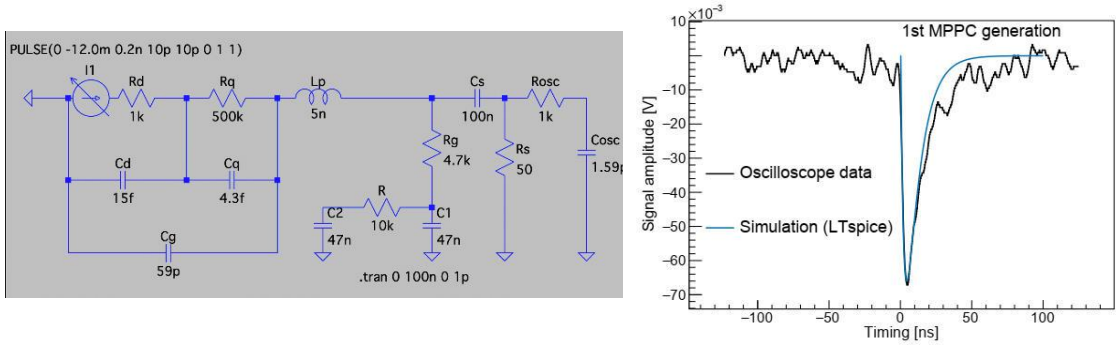

(a) (b)

Figure 4. (a) A simulated MPPC circuit for a 100 MHz bandwidth oscilloscope including Rosc and Cosc; (b) A good agreement between an observed MPPC waveform and a simulation

As studied in (Seifert et al., 2009), the MPPC signal, which is a discharge of the pixels when triggered by incoming photons, can be well-simulated with an equivalent electronic circuit implemented in the SPICE simulation program.[1] A simple but solid simulation of the MPPC is important for predicting the signal under the influence of other electronic components such as a low-pass filter, a high-pass filter, a shaping circuit, an amplifier, and the bandwidth of the signal reader. Based on the work with MPPC S10362-11–25 u (Seifert et al., 2009), we have developed a justified SPICE model presented on the left in Figure 4 for the MPPC S10362-13-050C. This simulation circuit is adapted to match our electronic circuit to provide the bias voltage and obtain the signal in Figure 3. In this model, an MPPC S10362-13-050C pixel can be modeled by a capacitor of Cd = 15 fF and a resistor of Rd = 1 kΩ. The quenching effect can be simulated by a capacitor of Cq = 4.3 fF and a resistor of Rq= 500 kΩ. The parasitic capacitance, which is strongly dependent on the number of pixels and their size, is adjusted to be Cg = 59 pF to fit our recorded waveform data well. In the operational voltage supply line, C1, C2, and R play the role of low-pass filter. Rg and Cs, on the other hand, play the role of a high-pass filter for the bias supply. The value of Cs, also known as the shaping capacitor, can affect the shape of the MPPC signal output. We used Cs = 100 nF in our signal readout circuit. The right side of Figure 4 shows the agreement between the MPPC signal recorded by a TBS1104 oscilloscope and our SPICE simulation of the MPPC electrical model. The effect of the 100 MHz bandwidth of the oscilloscope is included in the simulation, with Rosc = 1 kΩ and Cosc = 1.59 pF. The 50 Ω termination resistor of the oscilloscope is represented by Rs. It is worth noting that the pedestal line in the MPPC waveform data is not perfectly flat, which can be attributed to the imperfect grounding of our circuit. In the future, we intend to improve this effect and further explore our simulation model. Nevertheless, the result shown in Figure 4 indicates that we understand the functionality of the MPPC and the effects of the other electronic components relatively well.

With a large number of excellent features and a wide selection of product lines, MPPCs are applicable to various fields, including, but not limited to, extremely low-light detection in particle and nuclear physics, time-of-flight-based distance measurement for automobiles, fluorescence and chemiluminescence spectroscopy, biochemical sensors, single molecular detection, positron emission tomography in medical imaging systems, quantum computing, and cryptography.[2] In particle physics, mass production of MPPCs was first achieved in the T2K experiment (Yokoyama et al., 2010) in 2008 with approximately 60,000 MPPC pieces.

[1] http://bwrcs.eecs.berkeley.edu/Classes/IcBook/SPICE/

[2] https://www.hamamatsu.com/jp/en/product/optical-sensors/mppc/application/index.html

2. EXPERIMENTS

2.1. Characteristics of the MPPC under uncontrolled temperature conditions

2.1.1. Electrical gain

The electrical gain of an MPPC is defined as the number of charge carriers (electrons or holes) produced from an incident photon on a single MPPC pixel as

$$Gain = \frac{Q}{e} = \frac{C_{\text{pixel}} \times \left(V_{\text{op}} - V_{\text{bd}}\right)}{e}, \quad (1)$$

where Q is the output charge of avalanche multiplication, e = 1.602 x 10^{-19}, C is the elementary charge, C_{pixel} is the overall pixel capacitance, and V_{op} and V_{bd} are the operating and breakdown voltages of the MPPC, respectively. The overvoltage, defined as $\Delta V_{over} = V_{op} - V_{bd}$, is among the most important operational parameters of an MPPC. The electrical gain of the MPPC is expected to be linear with ΔV_{over} since the higher the overvoltage, the more ionization energy is available for the charge carriers. From Equation (1), with a pixel capacitance of C_{pixel} = 40 fF and an overvoltage of ΔV_{over} = 3V, an MPPC can attain an electrical gain of 7.5 x 10^5, which is a level similar to a photomultiplier tube (PMT).

At higher temperatures, the breakdown voltage increases because the lattice vibrations become stronger. Avalanche carriers are more likely to lose kinetic energy by scattering with the lattice atoms, reducing the ionization probability. As a result, the gain declines with an increase in temperature. Hence, to maintain a stable operation, it is often necessary to keep the MPPC in a temperature-controlled environment or to employ a temperature compensation circuit to adjust the reverse bias voltage automatically. However, in this study, we will examine the linearity of the MPPC electrical gain when the environmental conditions for MPPC operation are not tightly controlled.

- Measuring the electrical gain of the MPPC

To measure the electrical gain of the MPPC, a 430-nm-wavelength LED[3] is used as the light source. The light source is driven by a waveform generator, which is one of the functions of the Analog Discovery 2.[4] A reverse-biased voltage is supplied to the MPPC via a regulated low-noise DC power supply. The raw MPPC signal is then amplified by a factor of 100 using a NIM RPN-092 PM amplifier.[5] The amplified signal is synchronized with the output pulse from the generator used to control the LED light. After that, the signal is digitized with a DRS4 evaluation board (Ritt, 2018) and sent through a USB connection to a DAQ computer. The MPPC digitized pulses are integrated

[3] The wavelength is selected since it is close to the photon detection efficiency peak of the MPPC.

[4] https://digilent.com/reference/test-and-measurement/analog-discovery-2/start

[5] https://www.h-repic.co.jp/pdf/NIM_RPN_090-091.pdf

over a predefined timing window (about 100 ns), producing a charge histogram, as shown in Figure 5, for example. The integrated charge of each pulse is accumulated until there are sufficient statistics for the histogram. The histogram has peaks corresponding to the pedestal (readout noise), one p.e., two p.e., etc., pulses of the MPPC. The output charge equivalent to one incident photon is computed from the peak-to-peak interval between any two consecutive peaks, which are determined by fitting a multimodal Gaussian function to the charge histogram. The electrical gain is obtained from Equation (1), with corrections for using the NIM amplifier and the DRS4, and is calculated at various values of the overvoltage. The first MPPC generation, SC10362-13-050C, and the third MPPC generation, S13081-050CS (X1), are used to check the reliability and stability of the measurement.

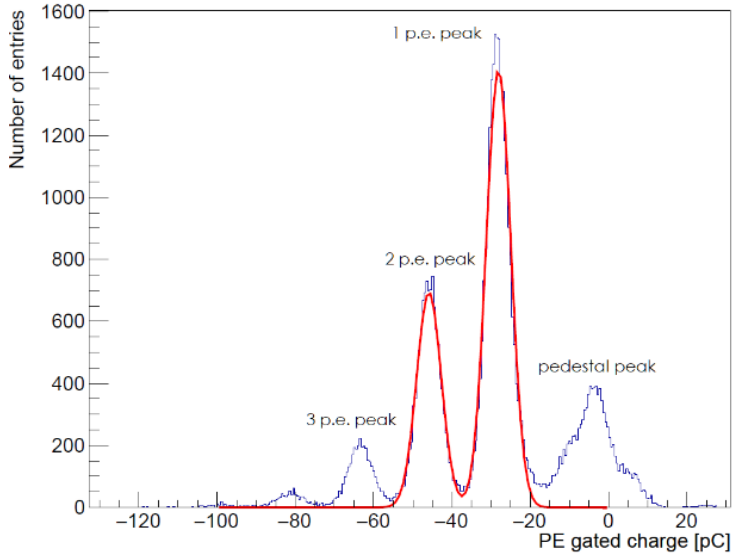

Figure 5. A typical charge histogram of a S13081-050CS(X1) MPPC operated at a given overvoltage

Notes: The charge histogram (blue line) is fitted with a multimodal Gaussian function (red line) to extract the electrical gain of the MPPC defined as the output charge equivalent to one photoelectron.

2.1.2. Thermal and optical noise

Three noise components are induced during MPPC operation: dark noise, crosstalk, and afterpulses.

- Dark noise

The so-called dark noise (Ghassemi et al., 2018) is randomly induced by the thermal excitation in the crystal lattice of the MPPC, producing signals indistinguishable from those of the photoelectric effect. The dark noise rate is proportional to the photosensitive area of the MPPC, the overvoltage, and temperature. Reducing the noise is of central importance in MPPC development since the MPPC is noisier than the vacuum-based photomultiplier. In experimental practice, the dark noise can be mitigated

by applying a trigger threshold that is significantly higher than the noise level. For extremely low-light measurements, such as the search for dark matter, the MPPC dark noise can be technically suppressed by operating the MPPC under cryogenic conditions.

- Afterpulses and optical crosstalk

In a given pixel, along with the genuine pulse triggered by the primary avalanche, the charge carriers, trapped in the same pixel or induced in a neighboring pixel, can avalanche a second pulse, called the afterpulse, or optical crosstalk. Both types of noise are characterized by the relative timing to the genuine pulse. If the afterpulses are released during the pixel's recovery, their amplitudes are smaller than the one p.e. pulse. On the other hand, if the afterpulse is avalanched after the pixel's recovery, its amplitude and shape are indistinguishable from that of a genuine pulse. Afterpulses can be observed on the trail of the left waveform shown in Figure 3. Prompt crosstalk, which happens simultaneously with the primary pulse, heightens the output charge since the pixels are connected in parallel. The two p.e. pulses observed in Figure 3 are likely due to crosstalk. In another scenario, the crosstalk pulse can be delayed and almost indistinguishable from the delayed afterpulse.

In this measurement, the dark count rates and prompt crosstalk of two generations of MPPC, the first generation SC10362-13-050C and the third generation S13081-050CS(X1), are measured. To minimize the effect of ambient light, the MPPC was placed inside an aluminum box and further covered with layers of black sheets. The dark noise rate, also known as the dark count rate, is defined as the discriminated pulse rate above a pre-set voltage threshold corresponding to a 0.5-p.e. pulse. The voltage threshold is determined according to the overvoltage. A regulated low-noise DC power supply, identical to the one used in the gain measurement, provides a high voltage for the MPPC. The NIM RPN 092 PM amplifies the MPPC signal by a factor of 100. The 0.5-p.e. amplified MPPC signals are registered by a NIM discriminator with an adjustable threshold. The 0.5-p.e. threshold is determined from the oscilloscope measurements. The logic pulses of the discriminator are fed through a NIM scaler to count the number of registered signals in a predefined time interval. When the measurement is conducted without any external light source, the rate of MPPC signal over the 0.5-p.e. threshold level is called the dark noise rate or dark count rate.

- Measuring the prompt crosstalk of the MPPC

The prompt crosstalk probability is estimated and measured using the same setup as the dark count rate measurement. Since we expect that a prompt crosstalk pulse superimposes more than one photon, the crosstalk probability (Ghassemi et al., 2018) is expressed as the ratio of dark count rate at 0.5 p.e. (trigged by dark noise) and 1.5 p.e. (triggered by optical crosstalk) threshold levels

$$Prompt\ crosstalk\ probability = \frac{Dark\ count\ rate\ at\ 1.5\ p.e.\ threshold\ level}{Dark\ count\ rate\ at\ 0.5\ p.e.\ threshold\ level}. \quad (2)$$

The signals with the 0.5 p.e and 1.5 p.e threshold levels are registered and counted using the discriminator and scaler, similar to the dark count rate measurement.

2.2. A tabletop cosmic ray detector with scintillator and MPPC

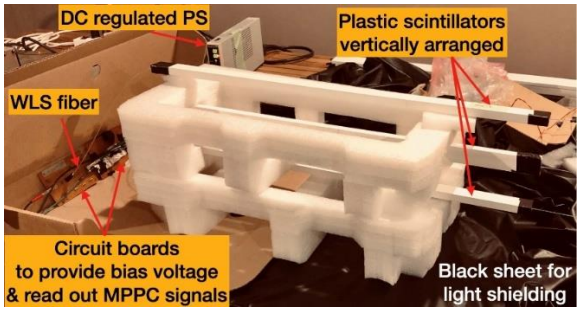

(a)

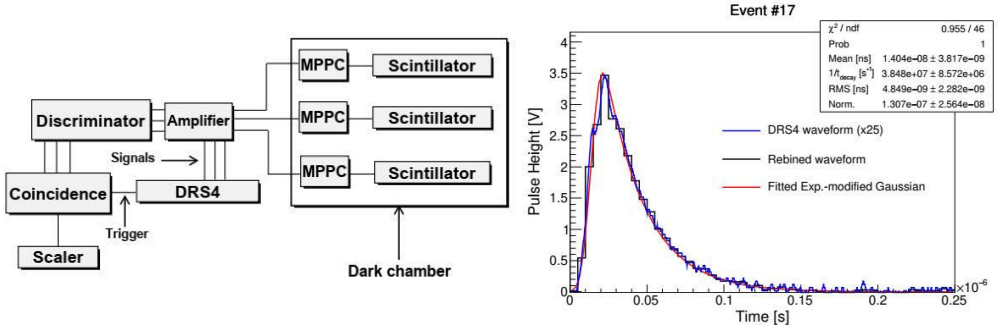

(b) (c)

Figure 6. (a) Our setup for cosmic ray measurement with key components highlighted; (b) A schematic diagram of the setup; (c) A waveform of scintillation photons collected by the MPPC when a cosmic ray passes through and deposits energy in the plastic scintillator

To demonstrate an MPPC application in particle and nuclear physics, we constructed a simple tabletop cosmic ray detector with a plastic scintillator, a wavelength shifting fiber (WLS), and the MPPC. A schematic diagram of the three-channel detector is shown in Figure 6b. Each channel is formed by one extruded 61 cm x 2.5 cm x 1.15 cm plastic scintillator[6] with a 2 mm-diameter hole in the middle to house the Y-11(200)-typed 1.2-diameter WLS fiber, which is coupled to a third generation MPPC, S13081-050CS(X1). When charged particles, such as muons, travel through the scintillator, they deposit energy and produce a flash of scintillation light (Leo, 1987). The WLS fiber collects these flashes of light and guides them to the MPPC for detection. The raw MPPC signal is then amplified by a factor of 10. A coincidence module eliminates the dark noise. A coincident signal of the top and bottom channels serves as a trigger to recognize whenever vertical cosmic rays are present and to acquire the middle one as a signal. A

[6] Considering an integrated cosmic ray flux of 1 $cm^{-2}min^{-1}$, 2.5 events per second is estimated with this setup. A smaller plastic scintillator can be used, but it needs more time to collect data to achieve the same statistics.

typical waveform of a cosmic ray-like signal is shown in Figure 6c. We investigated the MPPC response and decay time of the scintillation light by fitting the waveform to an exponential-modified Gaussian function.

The raw DRS4 waveform of the MPPC signal corresponding to the scintillation light created by the passage of a cosmic ray muon has a fine sampling and shows a relatively spiky pattern. To mitigate the possible effect on the fitting, we implemented a rebinning technique before carrying out a fit to extract the parameters of interest. The "rebinned" waveform has a larger pulse height than the raw waveform. In Figure 6, to make the two waveforms comparable, we scaled the DRS4 waveform by a factor of 25.

3. RESULTS AND DISCUSSION

3.1. Electrical gain

We measured the electrical gain with two different types of MPPC and at different overvoltages. Figure 7 shows that the electrical gains of the two MPPC generations vary linearly with the applied overvoltage. Notably, excellent linearity is achieved even when the environmental conditions are not tightly controlled. Also, we can have an electrical gain of ~1.5 x 10^6 if operating the MPPC with 3 V overvoltage. The results are corrected for the electronic gain from the NIM amplifier and the DRS4.

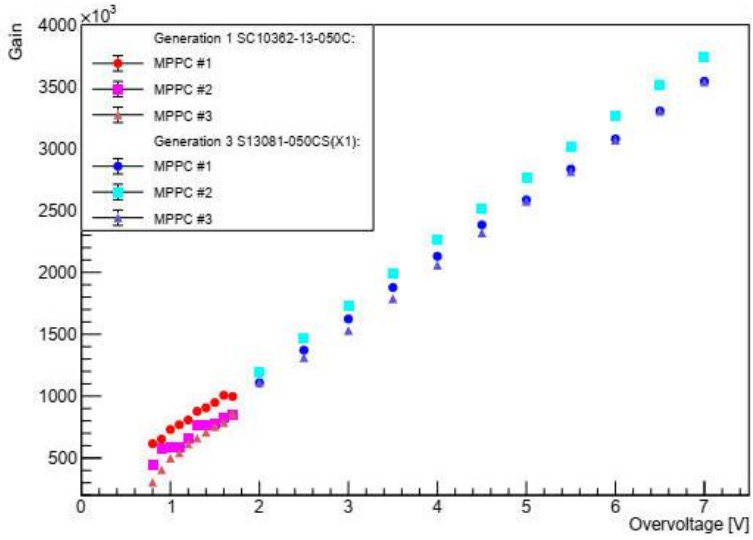

Figure 7. The electrical gains of three MPPCs (MPPC #1, MPPC #2, MPPC #3) from the first and third MPPC generations at different overvoltages

3.2. Dark noise rate and prompt crosstalk probability

We observed a difference in the dark count rates between the two MPPC generations (Figure 8). The dark count rate of the third MPPC generation is significantly lower than that of the first generation at the same overvoltage. For the first MPPC generation, SC10362-13-050C, as shown in the measurements, a high dark noise rate of

~ 1 MHz – 3.5 MHz was observed. The noise is suppressed significantly, by a factor of ~ 10, from the third MPPC generation, S13081-050CS(X1). Also, the dark count rates of MPPCs in the first generation, SC10362-13-050C, increase dramatically while the rates in the third generation, S13081-050CS(X1), rise gradually as a function of overvoltage, showing the better performance of the latter. The result concludes the excellent linearity of the dark noise rate on the overvoltage. For practical MPPC use, the trade-off between high electrical gain and low dark noise rate must be considered.

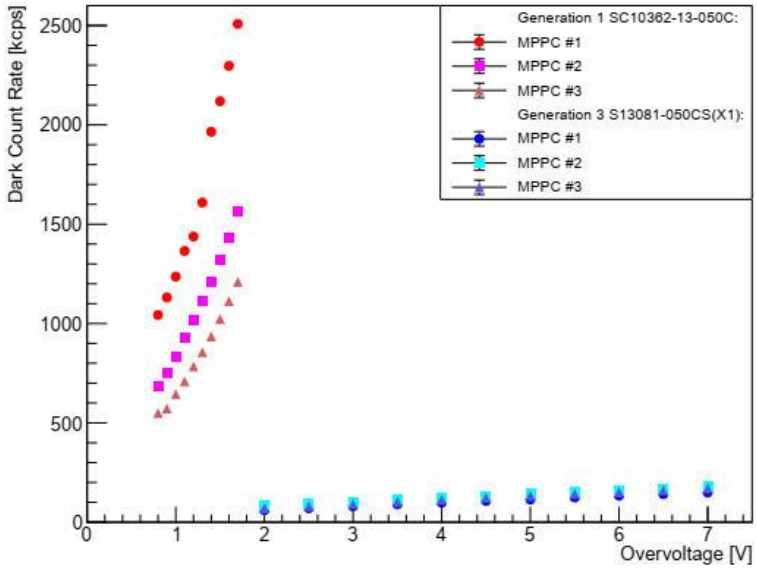

Figure 8. Measured dark count rate

Notes: Two MPPC generations and three MPPCs of each generation are used for comparison and consistency testing.

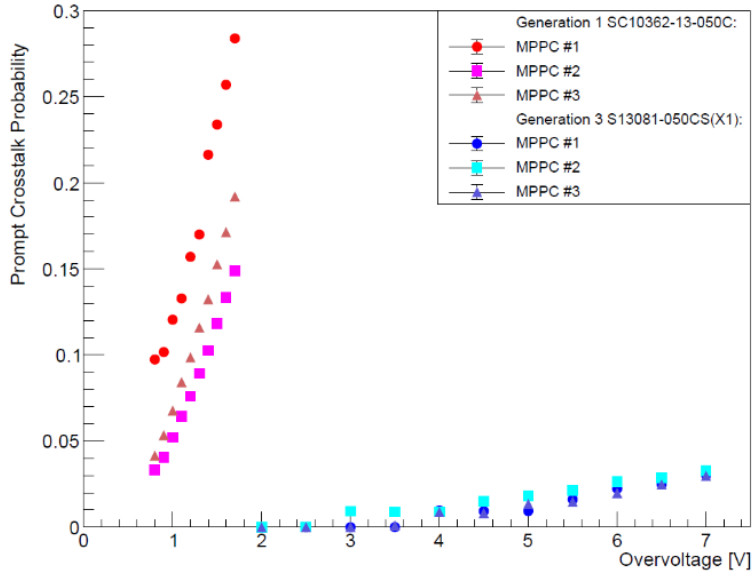

Figure 9. Prompt crosstalk probability as a function of overvoltage

The result illustrated in Figure 9 shows that the crosstalk probability of the two MPPC generations has the same behavior as the dark count rate. The crosstalk probabilities are about 10% – 30% in the first MPPC generation, SC10362-13-050C, and less than 5% in the third one, S13081-050CS(X1). This indicates that the third generation S13081-050CS(X1) crosstalk is significantly lower than in the first generation SC10362-13-050C.

3.3. Cosmic ray

The waveforms are fitted with an exponential-modified Gaussian to estimate the MPPC response and scintillation decay time, as shown in Figure 10. The fitted Gaussian width characterizes the MPPC response to the cosmic ray deposition and the fitted decay time shows how fast the scintillation light is produced. The results are shown in the plots of Figure 10. The Gaussian width is estimated at 6.25 $\pm$ 0.18 ns and the mean value of the fitted decay times is 27.63 $\pm$ 0.19 ns.

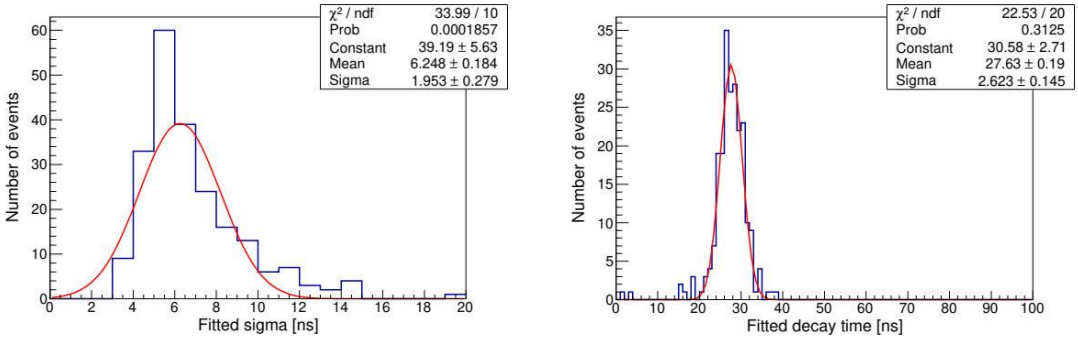

(a) (b)

Figure 10. (a) The distributions of the fitted Gaussian width (sigma); (b) Decay time to characterize the MPPC response and scintillation decay time

The MPPC pulses are integrated over a predefined timing window of around 100 ns, generating the output charges. The charge of the signal waveform and the gain of the MPPC are used to estimate the number of photoelectrons corresponding to the energy deposited by cosmic ray muons, which is about 2 MeV/cm on average (Groom et al., 2001). Figure 11 shows the distributions of the photoelectron number captured by the MPPC for two different widths of scintillator, 1.15 cm and 2.5 cm. We find that a Landau function does not provide a good fit to the distribution, but the convoluted Landau and Gaussian function does, affirming the fluctuation of the energy loss by charged particle ionization in a thin layer of material.

In Figure 11, the numbers of detected photoelectrons are 12.3 $\pm$ 5.1 and 31.1 $\pm$ 8.8 for the 1.15 cm-thick and 2.5 cm-thick scintillators, respectively. The result confirms that the energy deposited by the charged particles is proportional to the thickness of the scintillation material. Also, it shows that the number of photoelectrons detected when a cosmic ray passes through is well above the noise level. Thus, we conclude that an MPPC with a plastic scintillator is suitable for tracking charged particles in a laboratory room with loosely controlled environmental conditions.

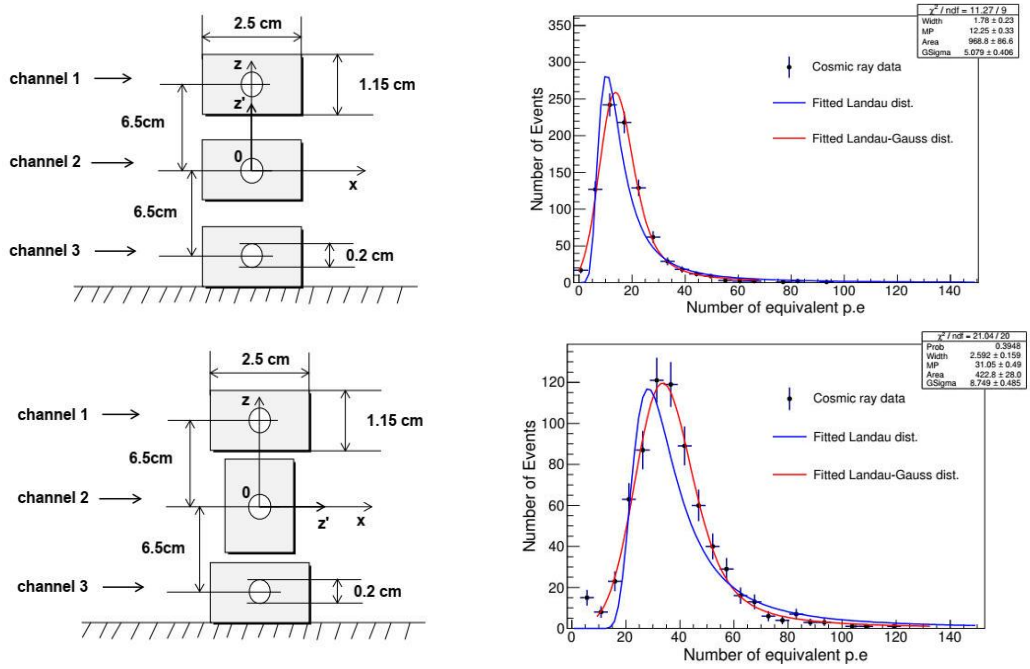

(a) (b)

Figure 11. (a) Schematic setups corresponding to the light yield (number of p.e.); (b) Distributions on 1.15 cm-thick and 2.5 cm-thick plastic scintillators

4. CONCLUSION

In this paper, we have introduced and measured the characteristics of an MPPC under loosely controlled conditions. We conclude that the MPPC performance is still stable and reliable enough for practical use even in such situations. Although the environmental conditions are not strictly controlled, our measurements of the electric gain, dark noise rate, and prompt crosstalk probability are in good agreement with the measurements in Hosomi (2016).

We also measured the scintillation light yield collected by the MPPC when cosmic rays pass through and deposit energy on the plastic scintillator. We observed more than ten photoelectrons per 2 MeV energy deposition, well above the background level. The results demonstrate that an MPPC can be used along with a ~ 1 cm or thicker plastic scintillator to construct a simple, cost-effective tabletop cosmic ray detector for educational and research purposes.

ACKNOWLEDGMENTS

We thank the High Energy Accelerator Research Organization (KEK), Japan, for supporting the electronics for the initiative to develop neutrino physics in Vietnam. The research is partly funded by the Vietnam National Foundation for Science and Technology Development (NAFOSTED) under grant number 103.99-2018.45.

REFERENCES

Ghassemi, A., Kobayashi, K., & Sato, K. (2018). *A technical guide to silicon photomultipliers* (*MPPC*) – *Overview*. Hamamatsu Photonics K. K. https://hub.hamamatsu.com/us/en/technical-notes/mppc-sipms/a-technical-guide-to-silicon-photomutlipliers-MPPC-overview.html

Groom, D. E., Mokhov, N. V., & Striganov, S. I. (2001). Muon stopping power and range tables 10 MeV–100 TeV. *Atomic Data and Nuclear Data Tables, 78*(2), 183-356. https://doi.org/10.1006/adnd.2001.0861

Hamamatsu Photonics. (2020). *Multi-pixel photon counters* (*MPPCs/SiPMs*). Hamamatsu Photonics K. K. https://www.hamamatsu.com/jp/en/product/optical-sensors/mppc/index.html

Hosomi, F. (2016). *Characterization of multi-pixel photon counters for a new neutrino detector*. https://hep.phys.s.u-tokyo.ac.jp/wp-content/uploads/2021/05/mth2016_hosomi.pdf

Leo, W. R. (1987). *Techniques for nuclear and particle physics experiments: A how-to approach.* Springer-Verlag. https://doi.org/10.1007/978-3-642-57920-2

Neamen, D. A. (2011). *Semiconductor physics and devices: Basic principles.* McGraw-Hill.

Ohashi, Y. (2019, November). *Current status of Hamamatsu Si detectors for collider experiments* [Paper presentation]. The Calorimetry for the High Energy Frontier 2019 Conference, Kyushu University, Japan. https://indico.cern.ch/event/818783/contributions/3598485/

Ritt, S. (2018). *DRS4 Evaluation Board User's Manual*. https://www.psi.ch/sites/default/files/2020-02/manual_rev51.pdf

Seifert, S., van Dam, H. T., Huizenga, J., Vinke, R., Dendooven, P., Lohner, H., & Schaart, D. R. (2009). Simulation of silicon photomultiplier signals. *IEEE Transactions on Nuclear Science*, *56*(6), 3726-3733. https://doi.org/10.1109/TNS.2009.2030728

Yamamoto, K., Nagano, T., Yamada, R., Ito, T., & Ohashi, Y. (2019). Recent development of MPPC at Hamamatsu for photon counting applications. *JPS Conference Proceedings*, *27*, 011001. https://doi.org/10.7566/JPSCP.27.011001

Yokoyama, M., Minamino, A., Gomi, S., Ieki, K., Nagai, N., Nakaya, T., Nitta, K., Orme, D., Otani, M., Murakami, T., Nakadaira, T., & Tanaka, M. (2010). Performance of multi-pixel photon counters for the T2K near detectors. *Nuclear Instruments and Methods in Physics Research Section A: Accelerators, Spectrometers, Detectors and Associated Equipment, 622*(3), 567-573. https://doi.org/10.1016/j.nima.2010.07.070